



Short communication

Two new Keggin-type polyoxometalate-based entangled coordination networks constructed from metal-organic chains with dangling arms



Xiu-Li Hao^{a,*}, Shi-Fang Jia^{a,*}, Yuan-Yuan Ma^b, Hong-Yi Wang^a, Yang-Guang Li^{b,*}

^a School of Chemical and Biological Engineering, Taiyuan University of Science and Technology, Taiyuan 030024, PR China

^b Key Laboratory of Polyoxometalate Science of Ministry of Education, Faculty of Chemistry, Northeast Normal University, Renmin Street No. 5268, Changchun, Jilin 130024, PR China

ARTICLE INFO

Article history:

Received 22 July 2016

Received in revised form 25 August 2016

Accepted 27 August 2016

Available online 28 August 2016

Keywords:

Polyoxometalate

Entangled coordination networks

Transition metal

Photocatalysis

ABSTRACT

Two new polyoxometalate(POM)-based entangled coordination networks with chemical formula of $[\text{Mn}_2(\text{H}_2\text{O})_2(\text{BBPTZ})_5][\text{SiW}_{12}\text{O}_{40}]$ (1) and $[\text{Ni}_2(\text{H}_2\text{O})_2(\text{BBPTZ})_5][\text{SiMo}_{12}\text{O}_{40}] \cdot 6\text{H}_2\text{O}$ (2) (BBPTZ = 4,4'-bis(1,2,4-triazol-1-ylmethyl)biphenyl), were prepared in a hydrothermal reaction system. Compounds 1–2 were characterized by elemental analyses, IR spectroscopy, thermogravimetric analysis, powder X-ray diffraction and single-crystal X-ray diffraction. In compound 1, dangling arms thread in quadrangular window of the adjacent 2-D layers, thus resulting in a rare 2-D → 3-D polythreading motif. Compound 2 exhibits a rare 2-D → 3-D zipper-closing motif. Using the degradation of methylene blue (MB) as the model, the photocatalytic activities of compounds 1–2 were investigated. Both compounds show efficient catalytic activity for the degradation of MB with the order of $2 > 1$. It is found that the POM species of compounds 1–2 play the main role in the photocatalytic degradation process.

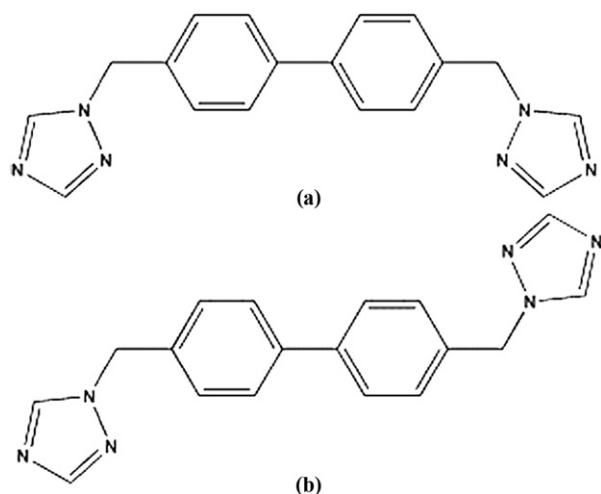
© 2016 Elsevier B.V. All rights reserved.

The design and synthesis of new organic-inorganic hybrid materials, especially polyoxometalate(POM)-based compounds modified by different transition-metals (TMs) and organic ligands, have attracted considerable attention over recent years, owing to not only their chemical and structural diversities but also their promising applications, such as adsorption, luminescence, catalysis, molecular recognition and electronic and magnetic materials [1]. In the field of catalysis, uniform dispersal of POM units within MOFs skeleton at the molecular level can improve POMs' specific surface area (SSA) to increase the catalytic activity, and they can be easily recycled after catalytic reactions [2]. In this aspect, POMs, as one type of unique nano-sized metal-oxo clusters, can be regarded as "building blocks" with their terminal or bridging oxides coordinating with metal cations [3]. Especially, Keggin-type POMs are best choice because of the following reasons: (i) the best chemically-tunable clusters with multiple components, negative charges and chemical modifications; (ii) having excellent catalytic properties, such as strong Brønsted acidity; (iii) their tuned acidic and redox properties [4]. Moreover, transition metal (TM) cations are important nodes due to their explicit coordination geometries and strong coordination ability to connect with POMs and organic ligands. However, the choice and design of organic ligands are of great importance for exploring new POM-based coordination networks [5–10]. From viewing coordination modes of

organic ligands, the monodentate N-donor ligands such as pyridine and imidazole groups have been employed due to their definite coordination modes with TM ions [5]. By comparison, the multi-dentate ligands such as triazole and tetrazole ligands have also been extensively explored in recent years considering their relatively high coordination activities with TM ions and various coordination modes [6–8]. Thus, the introduction of $-(\text{CH}_2)_n-$ and/or phenyl spacers between two terminal multi-dentate N-donor groups can generate flexible ligands with various coordination modes so as to construct more complicated and variable structural topologies [6–8]. Therefore, we chose a rigid and flexible double-triazole-containing ligand, namely 4,4'-bis(1,2,4-triazol-1-ylmethyl)biphenyl (BBPTZ) (see Scheme 1), and have successfully synthesized three new POM-based coordination networks [9] and a POM-encapsulating cationic MOF with wavelike channels [10]. As a continuing work of this reaction system, we introduce the metal ions Mn^{2+} and Ni^{2+} by changing pH to isolate two new Keggin-type polyoxometalate-based entangled coordination networks with the molecular formulas $[\text{Mn}_2(\text{H}_2\text{O})_2(\text{BBPTZ})_5][\text{SiW}_{12}\text{O}_{40}]$ (1) and $[\text{Ni}_2(\text{H}_2\text{O})_2(\text{BBPTZ})_5][\text{SiMo}_{12}\text{O}_{40}] \cdot 6\text{H}_2\text{O}$ (2) [11]. Interestingly, both compounds contain similar 2-D layers which are formed by Keggin-type POMs and ladder-like chains with dangling arms. Compound 1 exhibits a rare 2-D → 3-D polythreading network due to dangling arms threading in quadrangular window of the adjacent 2-D layers, but dangling arms of the adjacent 2-D layers are parallel with each other to display a rare 2-D → 3-D zipper-closing network for compound 2. Due to the excellent catalytic property of Keggin-type POMs, the photocatalytic properties of two compounds were also investigated.

* Corresponding authors.

E-mail addresses: haoxiuli1@163.com (X.-L. Hao), jjashifang@126.com (S.-F. Jia), liyig658@nenu.edu.cn (Y.-G. Li).



Scheme 1. Two configurations of BBPTZ (4,4'-bis(1,2,4-triazol-1-ylmethyl)biphenyl).

Single-crystal X-ray diffraction analyses [14] shows that compound **1** crystallizes in the monoclinic space group $P2(1)/c$. In **1**, the basic structural unit contains cationic $[\text{Mn}_2(\text{H}_2\text{O})_2(\text{BBPTZ})_5]^{4+}$ and the Keggin-type polyoxoanion $[\text{SiW}_{12}\text{O}_{40}]^{4-}$ (SiW_{12}) and two lattice water molecules (Fig. 1a and Fig. S1). In the cationic $[\text{Mn}_2(\text{H}_2\text{O})_2(\text{BBPTZ})_5]^{4+}$ unit, there is only one crystallographically independent Mn^{2+} center, which possesses a six-coordinated mode with four nitrogen atoms derived from four different BBPTZ ligands, one terminal oxygen atom originated from SiW_{12} polyoxoanions, and one coordinated water molecules (Fig. 1a and Fig. S1). The bond distances of $\text{Mn}-\text{N}$ vary from 2.204(2) Å to 2.244(2) Å, and $\text{Mn}-\text{O}$ are 2.192(1) Å and 2.237(1) Å. The bond angles of $\text{N}(\text{O})-\text{Mn}-\text{N}(\text{O})$ are in the range of 84.1(5)–173.9(6)°. It is interesting that the BBPTZ ligands can be regarded as three different types labeled with L_a , L_b and L_c as shown in Fig. 1a and Fig. S2. Although apical nitrogen atom of each triazole group on the L_a and L_b ligands displays a monodentate coordination mode with one Mn center, two rigid phenyl centers of L_a and L_b ligands with trans-configuration exhibit two different orientation (Fig. 1a and Fig. S2). For L_c ligand, apical nitrogen atom of one triazole group exhibits a monodentate coordination mode with one Mn center and the other triazole group is not coordinated with any atom (Fig. 1a and Fig. S2). Based on above coordination mode, the Mn atoms are connected via *trans*- L_a ligands to form an undulating 1-D chain and the *trans*- L_b can be viewed as the “middle rail” that connects the adjacent

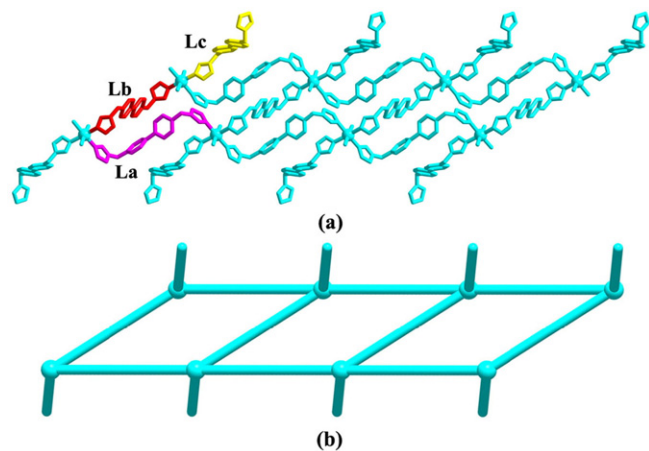


Fig. 1. (a) Ball-and-stick and (b) schematic views of the 1-D ladder-like chain with dangling arms in **1** formed by one Mn^{2+} center and BBPTZ ligands with three different kinds of structural configurations.

1-D chains to form a ladder-like chain (Fig. 1). Meanwhile, each Mn center also connects one S-type L_c ligand acted as “dangling arm” and L_c ligands protrude upper and lower sides of the ladder (Fig. 1). Further, the adjacent ladder-like chains are connected by the terminal O atom of the polyoxoanions to construct a 2-D network with quadrangle-like cavities, in which L_c ligands having an effectual length of about 16.3 Å are alternately appeared (Fig. 2 and Fig. S3). Such a 2-D network possesses two types of meshes (A and B) (Fig. 2). The A mesh is formed by four Ni centers, two L_a -type BBPTZ ligands and two L_b -type BBPTZ (Fig. 2a). The B mesh is constructed by four Ni centers, two L_a -type BBPTZ ligands and two SiW_{12} polyoxoanions (Fig. 2a). The sizes of two types of meshes are 15.33(1) × 16.31(5) Å and 14.67(1) × 16.31(5) Å, respectively (Fig. 2b). As a result, each B mesh is threaded by two dangling arms of above and below 2-D layers, thus resulting in a rare 2-D → 3-D polythreading motif (Fig. 3). In the packing arrangement, dangling arms of adjacent 2-D nets are extended in different directions, so that these adjacent 2-D nets are not parallel with each other, but these interval 2-D layers are parallel with each other (Fig. 3).

Single-crystal X-ray diffraction analysis [14] reveals compound **2** crystallizes in the triclinic space group $P-1$, and the crystallographically asymmetric unit consists of one Keggin-type polyoxoanion $[\text{SiMo}_{12}\text{O}_{40}]^{4-}$ (SiMo_{12}), two Ni^{2+} ion, three BBPTZ bridging ligands, two monoprotonated BBPTZ ligand, two coordinated water molecules and six lattice water molecule (Fig. 4a and Fig. S4). The cationic metal-organic fragment $[\text{Ni}_2(\text{H}_2\text{O})_2(\text{BBPTZ})_5]^{4+}$ contains one crystallographically independent Ni^{2+} center, which adopts a hexa-coordinated mode with four nitrogen atoms derived from four BBPTZ ligands, one terminal oxygen atom originated from SiMo_{12} polyoxoanions and one coordinated water molecules (Fig. 4a and Fig. S4). The bond lengths of $\text{Ni}-\text{N}$ range from 1.968(2) to 2.018(2) Å and the $\text{N}-\text{Ni}-\text{N}$ bond angles vary from 86.7(6) to 172.8(7)°. The bond distance of $\text{Ni}-\text{O}(12)$ is 2.478(1) Å, which can be viewed as weak coordination bonds between

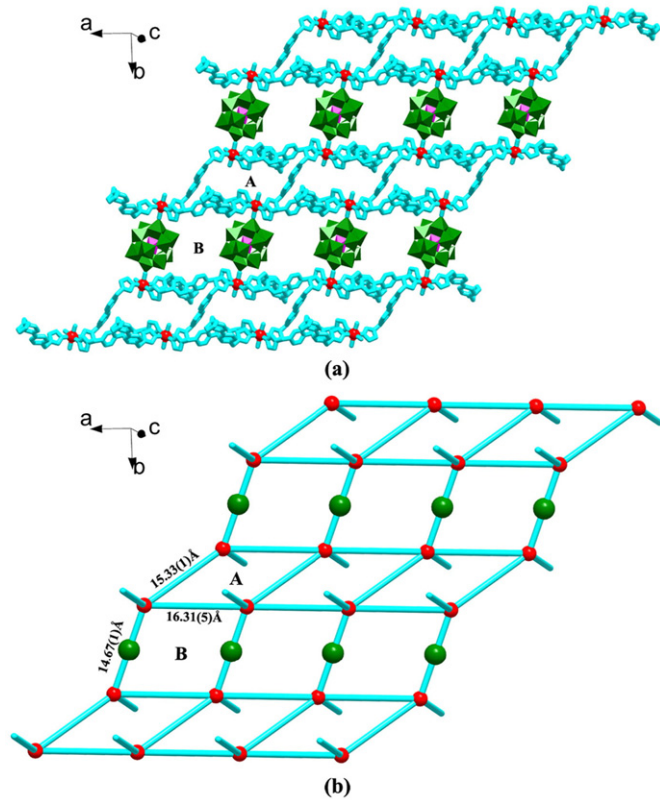


Fig. 2. (a) Structural views and (b) schematic views of 2-D network motif based on Keggin-type POM clusters and the ladder-like chains in **1** with two types of meshes (A and B).

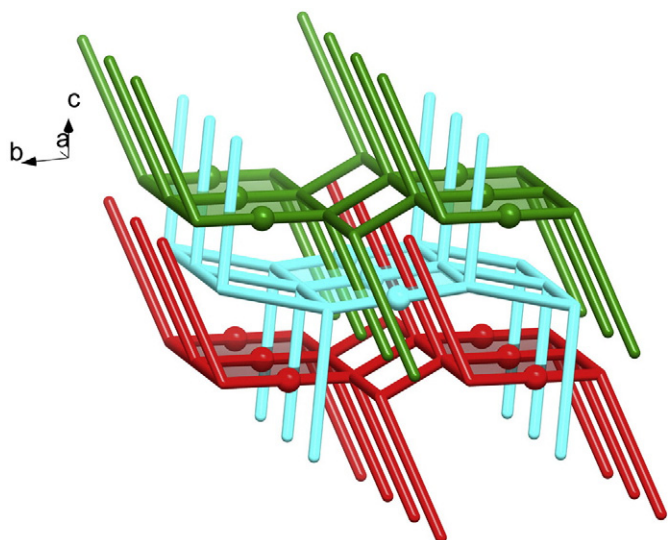


Fig. 3. Schematic illustration of 2-D \rightarrow 3-D polythreading motif of **1**, showing the mesh B threaded by two arms above and below.

Ni^{2+} center and the surface O atom of SiMo_{12} . It is noteworthy that the BBPTZ ligands in this metal-organic cationic moiety can be separated into three groups which are labeled with L_a , L_b and L_c (Fig. 4a and Fig. S5). The first group (L_a) possesses cis-configuration and links adjacent two Ni atoms into 1-D chains; the second group (L_b) displays trans-configuration and can be viewed as the “middle rail” that connects the adjacent 1-D chains to form a ladder-like chain; the third group (L_c) adopts trans-configuration and regards as “dangling arm”, protruding upper and lower sides of the ladder (Fig. 4 and Fig. S5). It is worth noting that the third group (L_c) is monoprotonated and only one triazole group coordinate with the Ni center. Furthermore, each POM unit acts as an inorganic linker to join the adjacent parallel 1-D ladder-like chains into a 2-D network with square meshes (Fig. 5). Compared with compound **1**, the 2-D layer of compound **2** also contains similar two kinds of meshes (A and B) with the sizes of $18.52(1) \times 16.76(3) \text{ \AA}$ and $15.29(9) \times 16.76(3) \text{ \AA}$, respectively (Fig. 5b). Note that the surface of 2-D layer is not flat due to existing the zipper-type structural feature and the adjacent 2-D layers are parallel with each other (Fig. 6). Thus, the adjacent 2-D layers are packed together through a “zipper-closing” mode, thus resulting in a rare 2-D \rightarrow 3-D zipper-closing motif (Fig. 6 and Fig. S6). Moreover, all the alternate dangling arms are well

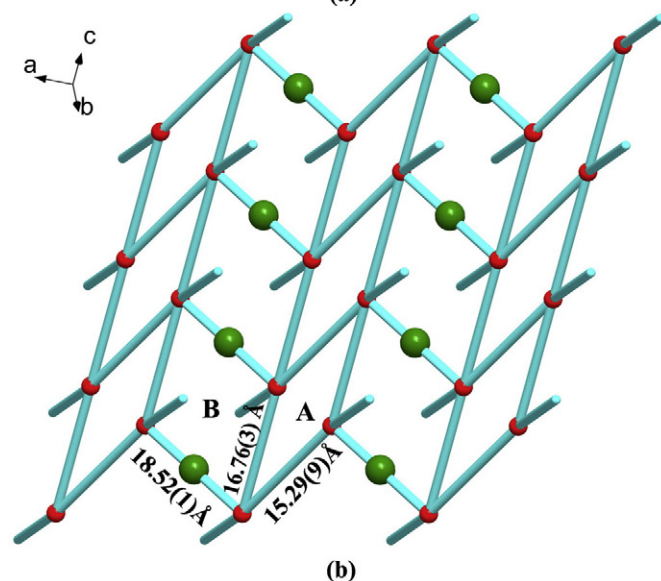
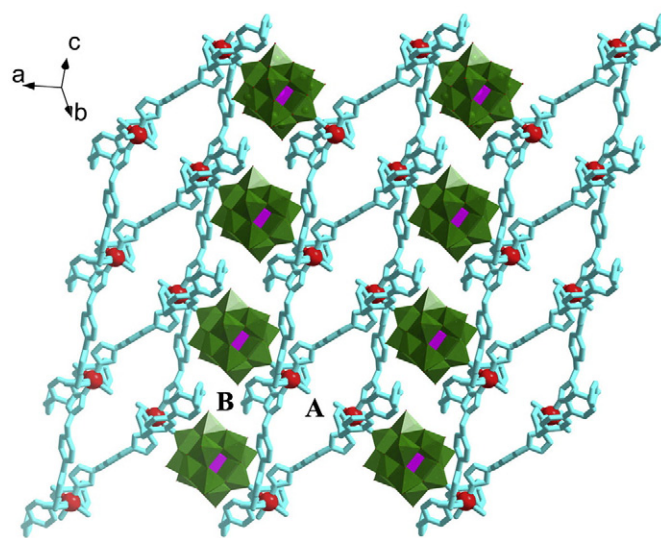


Fig. 5. (a) Polyhedral and ball-and-stick and (b) schematic views of the Keggin-type POMs-connected 2-D network of **2** with two kinds of meshes (A and B).

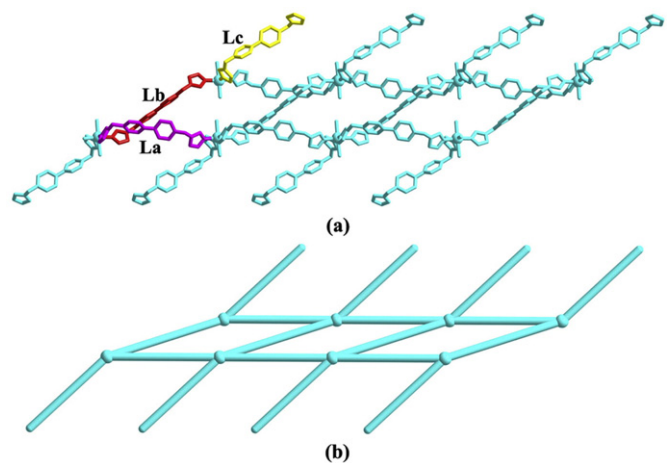


Fig. 4. (a) Ball-and-stick and (b) schematic views of the dangling arms-containing 1-D ladder-like chain in **2** based by one Ni^{2+} center and BBPTZ ligands with three different groups.

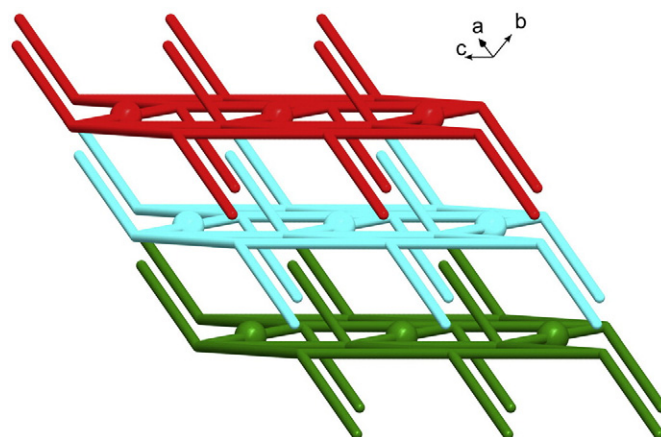


Fig. 6. Schematic illustration of 2-D \rightarrow 3-D zipper-closing motif of **2**, packing together through dangling arms of the adjacent 2-D layers.

separated in 3-D supramolecular framework without obvious intermolecular interactions.

Based on the above discussion, it is discovered that both compounds contain similar 2-D layers with two types of meshes and dangling arms. However, the structural features of their 2-D \rightarrow 3-D display obvious differences about the following reasons. Firstly, the dihedral angles between plane of dangling arms and the surface of 2-D layer are $74.3(6)$ and $39.6(8)^\circ$, respectively, which reveals that dangling arms of compound **1** trend to plumb the surface of 2-D layer (Fig. S7). In addition, orientations of dangling arms in adjacent 2-D nets exist the slight angle ($33.8(2)^\circ$) for compound **1**, but the adjacent 2-D layers containing dangling arms are parallel with each other in compound **2** (Fig. S8). Finally, the distance between the surfaces of adjacent 2-D layers is $9.70(2)$ Å less than the effectual length of dangling arm ($16.28(5)$ Å) in compound **1** (Fig. S9a). In compound **2**, the lengths of adjacent 2-D layers and dangling arm are $15.56(2)$ Å and $16.13(8)$ Å, respectively, which are extremely approximate (Fig. S9b). Therefore, dangling arms can thread meshes of the adjacent 2-D layers for compound **1**, but dangling arms of compound **2** only can parallelly and alternately appear (Figs. 3 and 6).

Nowadays the degradation of waste organic dyes is one of the currently significant tasks, since discharge of their waste can lead to serious water pollution and water eutrophication [16]. In this research field, the photocatalytic reaction by the use of photocatalysts under UV irradiation has been developed as an effective approach to decompose of organic materials. During the research process, methylene blue (MB) is usually employed as a typical model dye contaminant to evaluate the catalytic activities in purification of waste water. It is well known that a wide range of Keggin-type POMs have been demonstrated to be one type of potential photocatalysts in the degradation of organic dyes. It is worth mentioning that compounds **1–2** are insoluble in aqueous solution, thus they are employed as heterogeneous catalysts, which were investigated via the experimental model of MB photodegradation under UV irradiation. In a typical process, aqueous MB solution (400 mL, 10.0 mg L^{-1}) combining one of compounds **1–2** (50 mg) as the catalyst was exposed to UV light (125 W). Moreover, the photodegradation process of the blank MB aqueous solution without any catalyst was also monitored as a control experiment. Under UV irradiation, in contrast with the photodegradation process of MB without any photocatalyst, an obvious decrease in the absorption peaks of the MB solution monitored by UV-vis spectra was observed for compounds **1–2** (Fig. 7), indicating that both compounds possess excellent photocatalytic properties for MB degradation. As shown in Fig. 8, the plots of C_t/C_0 of MB solutions versus irradiation time further reveal that the photocatalytic activities increase from 33.37% (without any catalyst) to 93.22% for **1** and 97.45% for **2** after 90 min of irradiation.

In order to explore the active ingredient of compounds **1–2** in the catalytic process, the catalytic activity of the TM precursors (the mixture of $Mn(OAc)_2 \cdot 4H_2O/Ni(OAc)_2 \cdot 4H_2O$ and BBPTZ) and the POM precursors ($(Bu_4N)_4[SiW_{12}O_{40}]/(Bu_4N)_4[SiMo_{12}O_{40}]$) were respectively further performed as a series of comparative experiments. It is found that the catalytic activities of compounds **1–2** are a little higher than those of $(Bu_4N)_4[SiW_{12}O_{40}]$ and $(Bu_4N)_4[SiMo_{12}O_{40}]$ POMs, but the catalytic activities of the POM precursors exhibit obviously higher than the TM precursors (Fig. S10). Thus, the POM anions should be the catalytically active species in the photocatalytic decomposition of MB. This result is consistent with the reported catalytic mechanism of the POM species. As shown in Fig. S10, the catalytic activity of $(Bu_4N)_4[SiMo_{12}O_{40}]$ is slightly higher than that of $(Bu_4N)_4[SiW_{12}O_{40}]$. Similarly, the catalytic activities of compounds **1–2** are slightly different with the order of **2** (97.45%) $>$ **1** (93.22%). These catalytic differences between compounds **1–2** may be mainly derived from their difference in POM species. Furthermore, compound **2** exhibiting the highest catalytic activity was chosen as a representative catalyst to investigate catalyst lifetime. In our initial experiment, compound **2** recycled for five times also maintains the higher catalytic activity (Fig. S11). In comparison to the PXRD

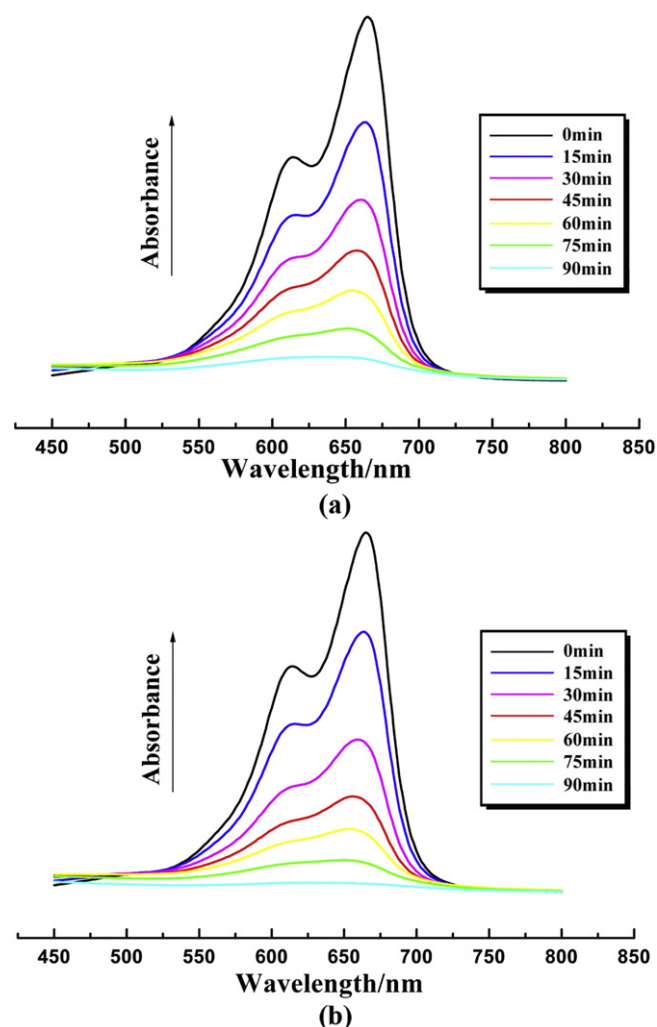


Fig. 7. UV-vis absorption spectra of the MB solutions during the decomposition reaction under UV light irradiation in the presence of compounds **1** (a) and **2** (b).

patterns of compound **2** before the catalytic process, PXRD pattern after five-cycle photocatalytic tests is still no obvious changes, further suggesting that such compounds **1–2** as heterogeneous catalysts are stable in the catalytic process (Fig. S12). Finally, a litter decrease in the absorption peaks of the MB solution was observed after 90 min without

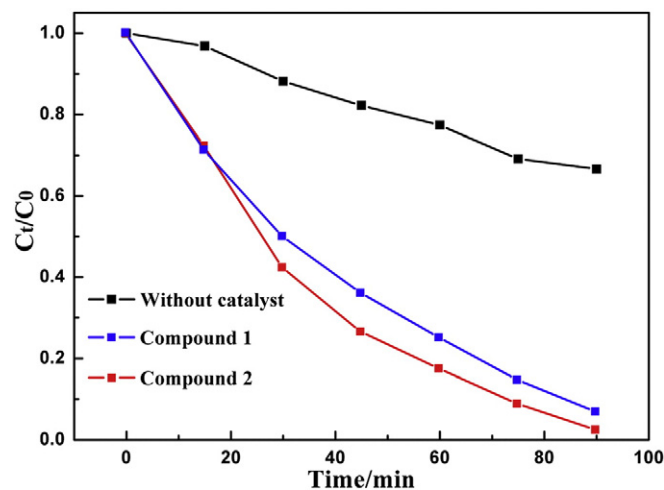


Fig. 8. Plot of C_t/C_0 of MB versus irradiation time under UV light in the presence of compounds **1** and **2**, and the black curve is the control experiment without any catalyst.

UV irradiation for compounds 1–2 (Fig. S13). It is proved that compounds 1–2 can only show effective catalytic activities under UV irradiation.

In summary, we presented two new entangled coordination networks based on Keggin-type polyoxometalates and metal-organic chains with dangling arms. It is found that both compounds contain similar 2-D layers with two types of meshes and dangling arms. Finally, compounds 1–2 exhibit the 2-D → 3-D polythreading motif and the 2-D → 3-D zipper-closing motif, respectively. In such a hydrothermal reaction system, only changing pH and transition metal cations can result in some slight differences of the structural features. Thus, based on the present work, it may be expected that the design of new double or multiple triazole-containing ligands, different metals and/or other POM precursors by changing pH may lead to more new POM-based metal-organic hybrid materials with desirable structures and functionalities in the future. This work is ongoing in our group.

Acknowledgments

This work was supported by Youth Foundation of Taiyuan University of Science and Technology (Grant 20143002), and the Start-up Foundation for Docotors of Taiyuan University of Science and Technology.

Appendix A. Supplementary material

CCDC numbers 1493116 for **1** and 1493117 for **2** contain the supplementary crystallographic data for this paper. These data can be obtained free of charge from the Cambridge Crystallographic Data Centre via www.ccdc.cam.ac.uk/data_request/cif. Supplementary data associated with this article can be found in the online version, at <http://dx.doi.org/10.1016/j.inoche.2016.08.013>.

References

- (a) D.Y. Du, J.S. Qin, Z.M. Su, Y.Q. Lan, Recent advances in porous polyoxometalate-based metal-organic framework materials, *Chem. Soc. Rev.* 43 (2014) 4615–4632;
- (b) Z.M. Zhang, T. Zhang, C. Wang, Z.K. Lin, L.S. Long, W.B. Lin, Photosensitizing metal-organic framework enabling visible-light-driven proton reduction by a Wells–Dawson-type polyoxometalate, *J. Am. Chem. Soc.* 137 (2015) 3197–3200;
- (c) H. Fu, C. Qin, Y. Lu, Z.M. Zhang, Y.G. Li, Z.M. Su, W.L. Li, E.B. Wang, An ionothermal synthetic approach to porous polyoxometalate-based metal-organic frameworks, *Angew. Chem. Int. Ed.* 51 (2012) 7985–7989;
- (d) F.J. Ma, S.X. Liu, C.Y. Sun, D.D. Liang, G.J. Ren, F. Wei, Y.G. Chen, Z.M. Su, A sodalite-type porous metal-organic framework with polyoxometalate templates: adsorption and decomposition of dimethyl methylphosphonate, *J. Am. Chem. Soc.* 133 (2011) 4178–4181;
- (e) J. Zhao, W.W. Dong, Y.P. Wu, Y.N. Wang, C. Wang, D.S. Li, Q.C. Zhang, Two (3,6)-connected porous metal-organic frameworks based on linear trinuclear $[\text{Co}_3(\text{COO})_6]$ and paddlewheel dinuclear $[\text{Cu}_2(\text{COO})_4]$ SBUs: gas adsorption, photocatalytic behaviour, and magnetic properties, *J. Mater. Chem. A* 3 (2015) 6962–6969;
- (f) D.S. Li, Y.P. Wu, J. Zhao, J. Zhang, J.Y. Luc, Metal-organic frameworks based upon non-zeotype 4-connected topology, *Coord. Chem. Rev.* 261 (2014) 1–27.
- (a) Q.X. Han, C. He, M. Zhao, B. Qi, J.Y. Niu, C.Y. Duan, Engineering chiral polyoxometalate hybrid metal-organic frameworks for asymmetric dihydroxylation of olefins, *J. Am. Chem. Soc.* 135 (2013) 10186–10189;
- (b) X.L. Hao, Y.Y. Ma, Y.H. Wang, F.C. Liu, Y.G. Li, New entangled coordination networks based on charge-tunable Keggin-type polyoxometalates, *Chem. Asian. J.* 9 (2014) 819–829;
- (c) C. Zou, Z.J. Zhang, X. Xu, Q.H. Gong, J. Li, C.D. Wu, A multifunctional organic-inorganic hybrid structure based on MnIII-porphyrin and polyoxometalate as a highly effective dye scavenger and heterogenous catalyst, *J. Am. Chem. Soc.* 134 (2012) 87–90;
- (d) X.L. Wang, Z.H. Chang, H.Y. Lin, A.X. Tian, G.C. Liu, J.W. Zhang, D.N. Liu, Effect of polyoxoanions and amide group coordination modes on the assembly of polyoxometalate-based metal-organic complexes constructed from a semi-rigid bis-pyridyl-bis-amide ligand, *CrystEngComm* 17 (2015) 895–903;
- (e) H.F. Hao, W.Z. Zhou, H.Y. Zang, H.Q. Tan, Y.F. Qi, Y.H. Wang, Y.G. Li, Keggin-type polyoxometalate-based metal-organic networks for photocatalytic dye degradation, *Chem. Asian. J.* 10 (2015) 1676–1683;
- (f) Y.Y. Ma, H.Q. Tan, Y.H. Wang, X.L. Hao, X.J. Feng, H.Y. Zang, Y.G. Li, Polyoxometalate-based metal-organic coordination networks for heterogeneous catalytic desulfurization, *CrystEngComm* 17 (2015) 7938–7947.
- (a) H.N. Miras, J. Yan, D.L. Long, L. Cronin, Engineering polyoxometalates with emergent properties, *Chem. Soc. Rev.* 41 (2012) 7403–7430;
- (b) A. Banerjee, B.S. Bassil, G.V. Rösenthaler, U. Kortz, Diphosphates and diphosphonates in polyoxometalate chemistry, *Chem. Soc. Rev.* 41 (2012) 7590–7604;
- (c) X.B. Han, Y.G. Li, Z.M. Zhang, H.Q. Tan, Y. Lu, E.B. Wang, Polyoxometalate-based nickel clusters as visible light-driven water oxidation catalysts, *J. Am. Chem. Soc.* 137 (2015) 5486–5493;
- (d) P. Putaj, F. Lefebvre, Polyoxometalates containing late transition and noble metal atoms, *Coord. Chem. Rev.* 255 (2011) 1642–1685;
- (e) X.B. Han, Z.M. Zhang, T. Zhang, Y.G. Li, W.B. Lin, W.S. You, Z.M. Su, E.B. Wang, Polyoxometalate-based cobalt-phosphate molecular catalysts for visible light-driven water oxidation, *J. Am. Chem. Soc.* 136 (2014) 5359–5366.
- M.T. Pope, *Heteropoly and Isopoly Oxometalates*, Springer, Berlin, 1983.
- (a) X.J. Yang, M. Sun, H.Y. Zang, Y.Y. Ma, X.J. Feng, H.Q. Tan, Y.H. Wang, Y.G. Li, Hybrid coordination networks constructed from e-Keggin-type polyoxometalates and rigid imidazole-based bridging ligands as new carriers for noble-metal catalysts, *Chem. Asian. J.* 11 (2016) 858–867;
- (b) Y. Hu, F. Luo, F.F. Dong, Design synthesis and photocatalytic activity of a novel lilac-like silver-vanadate hybrid solid based on dicyclic rings of $[\text{V}_4\text{O}_{12}]^{4-}$ with $\{\text{Ag}_7\}^{7+}$ cluster, *Chem. Commun.* 47 (2011) 761–763;
- (c) M. Zhu, S.Q. Su, X.Z. Song, Z.M. Hao, S.Y. Song, H.J. Zhang, A series of POM/Ag-based hybrids: distinct forms and assembly of $[\text{Ag}_x\text{Ly}]$ complexes through combinational effects of POM and isomeric ligands, *CrystEngComm* 14 (2012) 6452–6461.
- (a) J.Q. Sha, J.W. Sun, M.T. Li, C. Wang, G.M. Li, P.F. Yan, L.J. Sun, Secondary spacer modulated assembly of polyoxometalate based metal-organic frameworks, *Dalton Trans.* 42 (2013) 1667–1677;
- (b) X.F. Kuang, X.Y. Wu, R.M. Yu, J.P. Donahue, J.S. Huang, C.Z. Lu, Assembly of a metal-organic framework by sextuple intercatenation of discrete adamantane-like cages, *Nat. Chem.* 2 (2010) 461–465.
- (a) B. Liu, Z.T. Yu, J. Yang, W. Hua, Y.Y. Liu, J.F. Ma, First three-dimensional inorganic-organic hybrid material constructed from an “inverted Keggin” polyoxometalate and a copper (I)-organic complex, *Inorg. Chem.* 50 (2011) 8967–8972;
- (b) S.B. Li, L. Zhang, K.P. O’Halloran, H.Y. Ma, H.J. Pang, An unprecedented 3D POM-MOF based on (7,8)-connected twin Wells–Dawson clusters: synthesis, structure, electrocatalytic and photocatalytic properties, *Dalton Trans.* 44 (2015) 2062–2065;
- (c) H. Zhang, K. Yu, S. Gao, C.M. Wang, C.X. Wang, H.Y. Wang, B.B. Zhou, Two unusual organic-inorganic hybrid 3-D frameworks based on Keggin-type heteropoly blue anion-chains, 40-membered macrocycles, and sodium linker units, *CrystEngComm* 16 (2014) 8449–8456.
- (a) H. Fu, Y. Lu, Z.L. Wang, C. Liang, Z.M. Zhang, E.B. Wang, Three hybrid networks based on octamolybdate: ionothermal synthesis, structure and photocatalytic properties, *Dalton Trans.* 41 (2012) 4084–4090;
- (b) X.L. Hao, Y.Y. Ma, C. Zhang, Q. Wang, X. Cheng, Y.H. Wang, Y.G. Li, E.B. Wang, Assembly of new organic-inorganic hybrids based on copper-bis (triazole) complexes and Keggin-type polyoxometalates with different negative charges, *CrystEngComm* 14 (2012) 6573–6580;
- (c) X.L. Wang, X.J. Liu, A.X. Tian, J. Ying, H.Y. Lin, G.C. Liu, Q. Gao, A novel 2D → 3D $[\text{Co}_5\text{PW}_9]$ -based framework extended by semi-rigid bis (triazole) ligand, *Dalton Trans.* 41 (2012) 9587–9589.
- X.L. Hao, Y.Y. Ma, W.Z. Zhou, H.Y. Zang, Y.H. Wang, Y.G. Li, Polyoxometalate-based entangled coordination networks induced by an extended bis(triazole) ligand, *Chem. Asian. J.* 9 (2014) 3633–3640.
- X.L. Hao, Y.Y. Ma, H.Y. Zang, Y.H. Wang, Y.G. Li, E.B. Wang, A polyoxometalate-encapsulating cationic metal-organic framework as a heterogeneous catalyst for desulfurization, *Chem. Eur. J.* 21 (2015) 3778–3784.
- Synthesis of the ligand 4,4'-bis(1,2,4-triazol-1-ylmethyl)biphenyl (BBPTZ): the ligand BBPTZ was prepared according to the literature [12]. 1,2,4-triazole (1.38 g, 20 mmol) was dissolved in acetone (30 mL), and then PEG-400 (2 g), anhydrous potassium carbonate (5 g), and potassium iodide (0.5 g) were added to the above solution. After the solution was stirring for 30 min, 4,4'-bis(chloromethyl)biphenyl (2.5 g, 10 mmol) was added. The mixture was vigorously stirred and refluxed for 10 h. A white residue was obtained after filtering and distilling off the filtrate. The crude product was re-crystallized from hot water to give white crystalline product. Yield: 1.7 g (54%). Anal. Calcd for $\text{C}_{18}\text{H}_{16}\text{N}_6$: C, 68.34; H, 5.10; N, 26.56. Found: C, 68.26; H, 5.02; N, 25.50. IR (KBr)/ cm^{-1} : 3099(w), 1508s(s), 1269(s), 1140(s), 1014(s), 751(s). $[\text{Mn}_2(\text{H}_2\text{O})_2(\text{BBPTZ})_5][\text{SiW}_{12}\text{O}_{40}]$ (1): A mixture of $\alpha\text{-H}_4\text{SiW}_{12}\text{O}_{40} \cdot n\text{H}_2\text{O}$ [13] (0.225 g, 0.075 mmol), $\text{Mn}(\text{CH}_3\text{COO})_2 \cdot 4\text{H}_2\text{O}$ (0.0625 g, 0.25 mmol) and BBPTZ (0.1 g, 0.32 mmol) was dissolved in 10 mL of distilled water at room temperature and stirred for 0.5 h. The pH of the reaction mixture was adjusted to about 5.0 with 1.0 M NaOH. The suspension was sealed in a 23-mL Teflon-lined autoclave and heated at 140 °C for 3 days. After slow cooling to room temperature, yellow block crystals were filtered and washed with distilled water (65% yield based on W). Anal. Calcd for $\text{C}_{90}\text{H}_{84}\text{N}_{30}\text{O}_{42}\text{SiW}_{12}\text{Mn}_2$: C 23.47, H 1.83, N 9.13, W 47.98, Mn 2.39; Found: C 23.66, H 1.99, N 9.01, W 47.75, Mn 2.57. Selected IR (solid KBr pellet, cm^{-1}): 3444(s), 3136(w), 1610(w), 1498(m), 1435(m), 1402(w), 1274(m), 1184(w), 1128(s), 1014(s), 970(s), 922(s), 796(s). TG analysis shows that the first weight loss of 0.95% in the temperature range of 70–140 °C corresponds to two coordinated water molecules in **1** (calculated value 0.78%). $[\text{Ni}_2(\text{H}_2\text{O})_2(\text{BBPTZ})_5][\text{SiMo}_{12}\text{O}_{40}] \cdot 6\text{H}_2\text{O}$: A mixture of $\text{H}_4\text{SiMo}_{12}\text{O}_{40} \cdot n\text{H}_2\text{O}$ [12] (0.153 g, 0.075 mmol), $\text{Ni}(\text{OAc})_2 \cdot 4\text{H}_2\text{O}$ (0.0475 g, 0.25 mmol) and BBPTZ [13] (0.1 g, 0.32 mmol) was dissolved in 10 mL of distilled water at room temperature and stirred for 0.5 h. The pH of the reaction mixture was adjusted to about 3.0

with 1.0 M HCl. The suspension was sealed in a 23-mL Teflon-lined autoclave and heated at 140 °C for 3 days. After slow cooling to room temperature, green block crystals were filtered and washed with distilled water (60% yield based on Mo). Anal. Calcd for $C_{90}H_{96}N_{30}O_{48}SiMo_{12}Ni_2$: C, 29.48; H, 2.62; N, 11.47; Mo, 31.45; Ni, 3.20. Found: C, 29.69; H, 2.87; N, 11.25; Mo, 31.23; Ni, 3.35. Selected IR (KBr pellet, cm^{-1}): 3421(m), 3115(m), 1516(s), 1425(m), 1281(m), 1209(m), 1128(s), 1063(s), 962(s), 872(w), 800(s). TG analysis shows that the first weight loss of 4.02% in the temperature range of 75–140 °C corresponds to six lattice water molecules and two coordinated water molecules in **2** (calculated value 3.93%). Phase purity was confirmed by the powder X-ray diffraction (Fig. S18 and Fig. S19).

- [12] X.R. Meng, Y.L. Song, H.W. Hou, H.Y. Han, B. Xiao, Y.T. Fan, Y. Zhu, Hydrothermal syntheses, crystal structures, and characteristics of a series of Cd-btx coordination polymers (btx = 1,4-bis (triazol-1-ylmethyl) benzene), *Inorg. Chem.* 43 (2004) 3528–3536.
- [13] R.D. Claude, F. Michel, F. Raymonde, T. Rene, Vibrational investigations of polyoxometalates. 2. Evidence for anion-anion interactions in molybdenum(VI) and tungsten(VI) compounds related to the Keggin structure, *Inorg. Chem.* 22 (1983) 207–216.
- [14] Crystal data for **1**: $[Mn_2(H_2O)_2(BBPTZ)_5][SiW_{12}O_{40}]$, Mr = 4602.04, Monoclinic, space group P2(1)/c, a = 16.4732(9) Å, b = 22.7403(12) Å, c = 17.0098(9) Å, $\alpha = 90^\circ$, $\beta = 114.4260(10)^\circ$, $\gamma = 90^\circ$, V = 5801.6(5) Å³, Z = 2, Dc = 2.634 Mg·m⁻³, $\mu = 12.155$ mm⁻¹, $2.22 < \theta < 25.00^\circ$, F(000) = 4244, T = 298(2) K. 29928 reflection collected, 10206 unique. The final R₁ and wR₂ were 0.0526 and 0.0898, respectively [$I > 2\sigma(I)$]. Crystal data for **2**: $[Ni_2(H_2O)_2(BBPTZ)_5][SiMo_{12}O_{40}] \cdot 6H_2O$. Mr = 3662.76, triclinic, space group P-1,
- a = 14.008(3) Å, b = 15.408(3) Å, c = 16.763(3) Å, $\alpha = 98.52(3)^\circ$, $\beta = 92.34(3)^\circ$, $\gamma = 104.49(3)^\circ$, V = 3452.8(12) Å³, Z = 1, Dc = 1.761 Mg·m⁻³, $\mu = 1.410$ mm⁻¹, $3.01 < \theta < 25.00^\circ$, F(000) = 1804, T = 298(2) K. 26662 reflection collected, 11929 unique. The final R₁ and wR₂ were 0.0916 and 0.2511, respectively [$I > 2\sigma(I)$]. The crystallographic data were collected at 298(2) K on the Rigaku R-axis Rapid IP diffractometer using graphite monochromatic Mo K α radiation ($\lambda = 0.71073$ Å) and IP techniques. A multi-scan absorption correction was applied. The crystal data were solved by the direct method and refined by a full-matrix least-square method on F² using the SHELX-97 crystallographic software package [15]. All non-H atoms were refined anisotropically except the disordered solvent water molecules. However, some O atoms on the polyoxoanions and the C and N atoms on the organic ligands show ADP and NPD problems during the anisotropic refinements. Thus, the restrained command "ISOR" was used to restrain these non-H atoms. All above-restrained refinements led to relatively high restraint values for all compounds. H atoms on the C atoms were fixed in calculated positions. The H atoms on the lattice water molecules cannot be found from the weak residual peaks and were directly included in the final molecular formula. Selected bond lengths and angles of **1** and **2** are listed in Table S1 and S2.
- [15] (a) G.M. Sheldrick, SHELXS97, Program for Crystal Structure Solution, University of Göttingen, Göttingen, Germany, 1997;
(b) G.M. Sheldrick, SHELXL97, Program for Crystal Structure Refinement, University of Göttingen, Göttingen, Germany, 1997.
- [16] C.C. Chen, W. Zhao, P.X. Lei, J.C. Zhao, N. Serpone, Photosensitized degradation of dyes in polyoxometalate solutions versus TiO₂ dispersions under visible-light irradiation: mechanistic implications, *Chem. Eur. J.* 10 (2004) 1956–1965.